

Exosomes Secreted by M1-type Macrophages Improve Stress Urinary Incontinence by Promoting the Repair of the Levator ani Muscle Injury in Mice

Jianhong Cheng

Renmin Hospital of Wuhan University: Wuhan University Renmin Hospital

Shasha Hong

Renmin Hospital of Wuhan University: Wuhan University Renmin Hospital

Lian Yang

Renmin Hospital of Wuhan University: Wuhan University Renmin Hospital

Jianfeng Liu

Renmin Hospital of Wuhan University: Wuhan University Renmin Hospital

Li Hong (✉ dr_hongli@whu.edu.cn)

Renmin Hospital of Wuhan University

Research

Keywords: SUI, M1 type macrophages, exosomes, cyclic mechanical strain, C2C12 myoblasts

Posted Date: July 28th, 2021

DOI: <https://doi.org/10.21203/rs.3.rs-676443/v1>

License:   This work is licensed under a Creative Commons Attribution 4.0 International License.

[Read Full License](#)

Abstract

Background: Macrophages are involved in the regeneration of skeletal muscle injury and the exosomes secreted by a variety of cells promote the regeneration of tissues after injury. However, the potential effect of exosomes secreted by polarized macrophages on the repair of skeletal muscle after injury remains unclear. This study explored the effect of exosomes derived from M1 macrophages (M1-Exo) on the repair of levator ani muscle in mice after Vaginal Dilation (VD) modeling and the viability of C2C12 myoblasts after mechanical injury.

Methods: Differential ultracentrifugation was used to separate M1-Exo from 200 ng/mL lipopolysaccharide-induced polarization of M1 type macrophages culture medium. Nanoparticle tracking analysis, transmission electron microscopy, and western blotting of CD9 and Tsg101 proteins were employed to identify M1-Exo. *In vivo* experiment involving the vaginal balloon expansion method was used to simulate the trauma to the pelvic floor of the mouse during delivery. M1-Exo was injected into the levator ani muscle and its surroundings to detect the abdominal leak point pressure (ALPP) and the maximum bladder volume (MBV) of the VD mice at 3, 7, and 14 days. Then the levator ani muscle was taken for hematoxylin and eosin (H&E) staining to observe the muscle damage and repair. To evaluate the functional and anatomical recovery of M1-Exo on stress urinary incontinence (SUI) mice caused by VD model delivery trauma. Subsequently, an *in vitro* C2C12 myoblasts cyclic mechanical strain injury model was constructed to determine the best mechanical injury parameters. In the next step, through a series of *in vitro* functional tests, the effect of M1-Exo on the proliferation, senescence, and apoptosis of C2C12 myoblasts injured by cyclic mechanical strain was assessed. The effect of M1-Exo on the prevention and treatment of SUI caused by injury to the levator ani muscle after delivery was evaluated using animal experiments and cell-level studies.

Results: Powerlab software test results showed that the injection of M1-Exo into the levator ani muscle of SUI mice and its surroundings can significantly increase the mouse's ALPP, and MBV. H&E staining results revealed that M1-Exo can prevent secondary necrosis of broken muscle fibers, reduce nuclear migration of muscle fibers, maintain the shape of the muscle bundles, and promote normal muscle regeneration. CCK-8 proliferation reagent, senescence-associated β -galactosidase (SA- β -Gal) staining, and flow cytometry (PE/7-AAD staining) were used to determine the best *in vitro* simulation of the C212 myoblasts. The best damage parameters of the C2C12 myoblast injury model occurred at 5333 μ strain for a duration of 8 hours at 1 Hz. Subsequently, the test results of the CCK-8 proliferation reagent and EdU cell proliferation reagent suggested that M1-Exo promoted the proliferation of C2C12 myoblasts subjected to mechanically induced damage. SA- β -Gal staining results indicated that M1-Exo delayed the senescence of C2C12 myoblasts subjected to mechanically induced injury. Hoechst 33258 staining reagent and flow cytometry (PE/7-AAD staining) revealed that M1-Exo inhibited mechanically induced apoptosis of the C2C12 myoblasts.

Conclusions: Our experimental results established that M1-Exo helps in the functional and anatomical recovery of SUI mice caused by labor trauma. Furthermore, the findings imply that M1-Exo has a

protective effect on C2C12 myoblasts after cyclic mechanical strain damage, promotes their proliferation, delays aging, and inhibits apoptosis.

Background

Stress urinary incontinence (SUI) refers to uncontrolled leakage of urine from the external urethra when the abdominal pressure increases^[1]. Studies have reported that the prevalences of female SUI before and after pregnancy are 22.6% and 37.2%, respectively, and that it increases with the increase in gestational age, with the highest prevalence being observed in the third trimester^[2-4]. SUI induced by pregnancy and vaginal delivery is caused by damage to the pelvic floor muscles (mainly the levator ani muscle)^[5]. Therefore, it is necessary to repair the injured levator ani muscle promptly to reduce the occurrence of SUI.

Macrophages have become the main target of regenerative medicine owing to their unique plasticity^[6-8]. Macrophages quickly gather around the damaged area after skeletal muscle injury and regulate the functioning of muscle satellite cells by producing certain secretions^[9]. Inflammatory stimuli (such as bacterial components or gamma interferons) produce classically activated M1 macrophages, which can promote the proliferation of myoblasts^[10]. Furthermore, Pathol's animal experiments pointed out that exogenous M1 type macrophages therapy can reduce post-traumatic muscle fibrosis and enhance muscle fiber regeneration^[11]. M1-type macrophages have a positive effect on the regeneration of skeletal muscles after an injury. However, owing to the plasticity of macrophages, cell therapy based on M1 macrophages is particularly vulnerable to phenotypic control issues. For example, when M1-type macrophages are implanted in the body, it is not clear whether the phenotype of exogenously stimulated M1-type macrophages can be maintained. Therefore, for cell therapy based on M1 macrophages to be clinically feasible, it is necessary to find ways to ensure their stable functioning *in vivo*.

Exosomes are lipid vesicles with a diameter of 30–150 nm and are derived from the endosomal system. These vesicles are miniature versions of the parent cells and carry many biomolecules present in the parent cells, such as nucleic acids, proteins, and lipids^[12, 13]. Exosomes not only reflect the characteristics of the donor cells but also perform specific functions in the recipient cells^[14]. Therefore, this study employed M1-type macrophages-derived exosomes to conduct experiments that can solve the problem of phenotype maintenance of these macrophages *in vivo* transplantation treatment. The vaginal balloon expansion method was used to simulate the damage to the levator ani muscle during childbirth in mice^[15] and to explore whether the injection of M1 macrophages-derived exosomes around the injured site can promote muscle repair and improve the symptoms of SUI. In addition, this study examined the effect of these exosomes on the viability of myoblasts after cyclic mechanical stress injury at the cellular level.

Results

CMS causes C2C12 myoblast damage

A four-point bending cell mechanics loading instrument was used to mechanically load the C2C12 myoblasts. The strain applied was 0, 1333, 2666, and 5333 μ strain, the strain-time was set to 0, 4, 8, and 12 h, and the frequency was 1 Hz. After mechanical induction, the C2C12 myoblasts were cultured in an incubator for another 4 h, and the cell viability was measured using CCK-8. As shown in Figure 1A, the results were compared to those of the control group. When the mechanical strain was 5333 μ strain, the cell activity decreased most obviously, and the activity fell gradually with the increase in strain application time. However, when the strain was 1333 μ strain, there was no statistically difference in cell viability ($p > 0.05$). In addition, when the mechanical strain was 2666 μ strain for 12 h, the cell activity was also significantly reduced ($p < 0.001$). Nevertheless, because the application time was too long, the probability of cell contamination increased and the damaging effect was less than that of the strain of 5333 μ strain. Hence, this experiment selected 5333 μ strain of the CMS as the optimal parameter.

To further investigate the effect of mechanical strain on the senescence and apoptosis of C2C12 myoblasts, the CMS parameter was set to 5333 μ strain, the CMS time was set to 0, 4, 8, and 12 h, the frequency was set to 1 Hz, and the CMS mode was loaded. In C2C12 myoblasts, a β -galactosidase staining kit was used to detect cell senescence. When compared with the control group, SA- β -Gal positive cells increased significantly in the 8-h group, while a large number of cells changed morphology in the 12-h group (Figure 1B). At the same time, the apoptosis test results revealed that when compared with the cells in the control group, the apoptosis rate in the 8-h group was about 30%, while the proportion of apoptotic cells in the 12-h group was too high (Figure 1C, D). Therefore, the best parameters of the C2C12 myoblast injury model occurred at 5333 μ strain for a duration of 8 hours at 1 Hz in this study. The above results indicate that a C2C12 myoblast injury model induced by cyclic mechanical strain has been successfully constructed and that a certain degree of mechanical strain can inhibit the proliferation of the myoblasts and promote their senescence and apoptosis.

Isolation and characterization of M1-Exo

Differential ultracentrifugation was used to extract M1-Exo; their characteristics are depicted in Figure 2. Nanoparticle tracking analysis showed that the diameter of the extracted vesicles was 81.3 nm (Figure 2A). Transmission electron microscopy demonstrated the presence of scattered oval or round vesicles. Their average particle size was 30–150 nm (Figure 2B). Furthermore, western blot results suggested that the protein extracted from the M1 macrophages contained almost no exosomal markers CD9 and Tsg101, while the exosomal group was positively expressed (Figure 2C). The above results signify the successful extraction of M1-Exo..

M1-Exo promote the repair of the levator ani muscle in SUI mice and improves the urodynamic parameters

Thirty-six mice with a positive sneeze test and a significant decrease in urodynamic parameters (ALPP and MBV) one day after the injury were included in the SUI model. ALPP and MBV were measured 3, 7, and 14 days after injection of M1-Exo or saline. In this study, the ALPP and MBV of normal mice were 40.02 ± 2.38 cmH₂O (Figures 3A-c, A-f, A-g) and 101 ± 5 μ L (Figure 3C), respectively. After the levator ani muscle was injured, the urodynamic parameters were significantly reduced (Figures 3A-a, B; C). When compared with the SUI group not injected with M1-Exo, the ALPP and MBV of the mice in the M1-Exo group improved considerably, and there were significant differences (Figures 3A, B, C). On the 14th day, the ALPP and MBV values of the SUI+M1-Exo group were not statistically different from those of the normal group (Figures 2B, C). These findings suggest that M1-Exo can completely restore ALPP and MBV within 14 days.

Levator ani muscle injury is an important cause of SUI [16, 17]. In the control group, the levator ani muscle fibers of the mice were dyed uniformly pink when examined microscopically, and the muscle cell nucleus was oval. Multiple nuclei were present around each muscle fiber, close to the inner surface of the muscle membrane, and the fibers were closely connected to form a bundle (Figure 3D-d). Once the levator ani muscle is injured, the muscle bundles are disordered, the size and shape of the muscle fibers are irregular, inflammatory cells are infiltrated, and a large number of pathological nuclei are seen in the muscle fibers (Figures 3D-a, D-b, D-c). The SUI group displayed muscle fiber rupture accompanied by necrosis and atrophy during the repair process, and inflammatory cell infiltration was observed. Besides, the neonatal muscle fiber morphology was irregular, and atrophy was accompanied by compensatory hypertrophy (Figures 3D-a, D-b, D-c). M1-Exo prevented secondary necrosis of the broken muscle fibers, maintained the shape of the muscle bundles, and promoted normal muscle regeneration. (Figures 3D-e, D-f, D-g). In addition, decreased nuclear translocation was observed in the SUI+M1-Exo group (Figures 3D-a, D-e).

M1-Exo promotes the proliferation of C2C12 myoblasts injured by CMS

C2C12 myoblasts were cultured at a mechanical force of 5333 μ strain and a force-frequency of 1 Hz, 8 h after loading. The cells were then cultured for 4 h and supplemented with 1×10^{10} particles/mL exosomes or PBS for 12 h, 24 h, and 36 h. CCK-8 kit was used to detect the proliferation level of the injured C2C12 myoblasts. As shown in Figure 3A, when compared with control group, the proliferation ability of the C2C12 myoblasts was significantly reduced after 8 h of mechanical force loading-induced injury. However, after culturing in DMEM medium with M1-Exo for 24 h, the proliferation level of the injured C2C12 myoblasts increased ($p < 0.01$). Furthermore, after the M1-Exos were cultured for 36 h, the injured C2C12 myoblasts almost returned to the normal proliferation level (Figure 3A).

The injured C2C12 myoblasts were cultured in DMEM medium with 1×10^{10} particles/mL of M1-Exo for 24 h. Subsequently, their proliferation rate was detected by using the EdU kit. The results showed changes similar to CCK-8, further confirming that the proliferation rate of the C2C12 myoblasts after mechanical damage was significantly increased as a result of co-culturing with M1-Exo (45.0%, $p < 0.001$ vs. -Exo

group) (Figures 5B, C). The results prove that M1-Exo promotes the proliferation of C2C12 myoblasts damaged by cyclic mechanical strain.

M1-Exo delays the senescence of C2C12 myoblasts injured by CMS

After the C2C12 myoblasts were treated in the above-mentioned manner, the β -galactosidase staining kit was used to detect their degree of senescence. In this experiment, the expression levels of β -galactosidase in the C2C12 myoblasts treated under different conditions tended to vary. As shown in Figure 4, when compared with the undamaged control group, the positive staining rate of the C2C12 myoblasts subjected to mechanically induced injury was significantly higher ($p < 0.05$), but the 1×10^{10} particles/mL of M1-Exo intervention lowered the positive staining rate. After 24 h, the positively stained C2C12 myoblasts of SA- β -Gal were significantly reduced and were closer to those of the undamaged control group. Therefore, it can be inferred that M1-Exo can delay the senescence of the damaged C2C12 myoblasts induced by cyclic mechanical strain.

M1-Exo inhibits the apoptosis of C2C12 myoblasts injured by CMS

After the C2C12 myoblasts were treated in the above manner, the Hoechst 33258 staining kit was used to detect the degree of apoptosis. As shown in Figures 5A and B, the C2C12 myoblasts subjected to injury induced by mechanical force had more bright blue fluorescence and condensed nuclei than the normal undamaged control group. After the intervention with M1-Exo, the number of bright blue fluorescence and condensed nuclei decreased significantly. Moreover, flow cytometry was used to detect the apoptosis rate of the C2C12 myoblasts after mechanical damage, and the results showed changes similar to Hoechst 33258 staining. These findings confirmed that the apoptosis rate of the C2C12 myoblasts after mechanical damage increased significantly (30.0%, $p < 0.001$ vs. control group). However, after co-cultivation with M1-Exo, the apoptosis rate was reduced to 12.0% (Figures 5C, D). The results validate that M1-Exo can inhibit the apoptosis of C2C12 myoblasts induced by cyclic mechanical strain.

Discussion

American scholar Delancey put forward the "Hammock Hypothesis," which states that the main supporting parts of the urethra and bladder neck are the complete vaginal wall at the bottom of the bladder and the pelvic fascia. The levator muscles contract, tighten the vaginal wall and pelvic fascia structure, flatten the urethra, and increase the internal pressure of the urethra, thereby effectively resisting the increased intra-abdominal pressure and controlling the discharge of urine. If these supporting "hammocks" are destroyed and the abdominal pressure increases, the urethra cannot be closed normally, resulting in SUI.

The levator ani is a pair of thick muscles. The muscles on both sides are symmetrical to each other and gather downward and inward into a funnel. The levator ani is composed of the pubococcygeus muscle, the iliococcygeus muscle, and the sitting tail muscle. Abdominal pressure can be transmitted to the pelvis through mechanics and acts on the levator ani muscle that closes the pelvis. If the pressure exerted on these muscles during delivery exceeds their physiological tolerance, injury occurs. Levator ani muscle injury is considered to be one of the key factors for SUI^[18]. Research data show that among American women, the rate of levator ani injury during vaginal delivery of primipara is as high as 5–33%, and with the use of obstetrical forceps, the rate of injury increases to 63.15%^[19, 20]. At present, there are many clinical methods to treat SUI, such as pelvic floor muscle training^[21], electrical stimulation^[22], and surgical treatment^[23]; nevertheless, the cure rate needs to be improved. Therefore, it is pertinent to explore new and effective therapeutic approaches. Exosomes, a kind of nanovesicles secreted by cells, participate in the biological processes of the target cells by transmitting material information such as DNA, RNA, and proteins^[24]. Studies have shown that in a variety of diseases, some specific molecules contained in exosomes may serve as potential therapeutic targets^[25–28]. Hence, exosomes have immense potential in the diagnosis and treatment of clinical diseases. This study has explored the preventive and therapeutic role of M1-Exo in levator ani muscle injury caused by vaginal delivery and the occurrence of SUI in women.

In this study, a mechanical force-induced C2C12 myoblast injury model was first constructed. The four-point bending cell mechanical loading system was used to load mouse C2C12 myoblasts at a fixed frequency of 1 Hz. It was found that under 1333 μ strain, no significant changes were found in cell activity ($p > 0.05$). However, when the applied force was increased to 5333 μ strain, the activity of the C2C12 myoblasts decreased significantly ($p < 0.001$), and the cell survival rate gradually decreased with time. In addition, using a smaller mechanical force while loading and prolonging the action time led to increased cell damage. For example, when the force was 2666 μ strain and the time was 12 h, the cell survival rate lowered significantly ($p < 0.001$), but the damaging effect was less than that in the 5333 μ strain group under the same conditions. It could be concluded that the system can cause cell damage, and as the mechanical force is increased and the time is prolonged, the degree of cell damage increases. Therefore, cell damage can be increased by applying a low loading force and prolonging the time of application or by increasing the loading force to obtain appropriate cell damage within a short time. However, loading with an strain time of > 10 h significantly accentuated the cell damage. There is a probability of pollution; hence, the strain selected in this study was 5333 μ strain. Moreover, to further confirm that the device did cause damage to the C2C12 myoblasts, cell apoptosis and senescence were measured at different time points when the force was 5333 μ strain. When the loading time was 12 h, the cell apoptosis rate was too high and there were several morphological changes. Besides, the cells were in a state of excessive damage, which is not suitable as a research model. Therefore, the best damage condition under this device was found to be 5333 μ strain, with added force and force-time of 8 h. Cell proliferation experiments also showed that the mechanical force under the above conditions significantly reduced the proliferation activity of the C2C12 myoblasts.

The construction of the mouse model by the transvaginal balloon expansion method is based on the mechanical damage to the pelvic floor tissue caused by pregnancy and childbirth. The method is simple to operate, has good reproducibility, causes little damage to the mice, and has a high postoperative survival rate, which is suitable for use in research. Subsequently, the exosomes were separated from the M1 macrophages supernatant by differential ultracentrifugation. A certain amount of M1-Exos was injected locally into the levator ani muscle of the SUI mice and its surroundings after 3, 7, and 14 days of routine rearing. Powerlab software was used to detect the changes in urodynamic parameters (ALPP, MBV), and the damage and repair status of the levator ani muscle was observed by H&E staining. The results confirmed that M1-Exo can prevent secondary necrosis of the broken muscle fibers, maintain the shape of the muscle bundles, and promote normal muscle regeneration (Figs. 3D-e, D-f, and D-g). Besides, decreased nuclear translocation was seen in the SUI + M1-Exo group (Fig. 3D-a, D-e).

Finally, M1-Exos were co-cultured with C2C12 myoblasts that were damaged by mechanical force. The results confirmed that M1-Exo could significantly decrease the damage to the C2C12 myoblasts induced by mechanical force, promote the proliferation of C2C12 myoblasts, and significantly inhibit cell apoptosis and senescence. However, this study has certain limitations. Although it has been confirmed that M1-Exos have a potential therapeutic effect on the injured C2C12 myoblasts, the specific regulatory mechanism is yet to be elucidated.

Conclusions

In summary, our results show that M1-Exos serve as functional vesicles. They can promote the proliferation of C2C12 myoblasts after mechanical injury, delay their senescence, and inhibit their apoptosis. M1-Exo has a significant protective effect on the vitality of C2C12 myoblasts, thereby alleviating simulated childbirth trauma and urinary incontinence in post-SUI mice and accelerating the repair of the levator ani muscle.

Materials And Methods

Cell culture and reagents

Mouse RAW264.7 macrophages were purchased from Wuhan Magall Biotechnology Co., Ltd. (introduced by the Chinese Academy of Sciences), and mouse C2C12 myoblasts were procured from Nanjing Kebai Biotechnology Co., Ltd. Both RAW264.7 macrophages and C2C12 myoblasts were maintained in high glucose Dulbecco's Modified Eagle's Medium (DMEM) (Genom Biotech Co. Ltd., Hangzhou, China) supplemented with 10% fetal bovine serum (FBS) (Gemini Bio-Products, Fisher Scientific, Waltham, MA, USA) and 1% penicillin and streptomycin (Beyotime Biotech Co. Ltd., Suzhou, China). The cells were cultured in a humidified incubator (Thermo Fisher Scientific, Waltham, MA, USA) at 37°C with 5% CO₂.

When the growth density of RAW264.7 macrophages reached about 90%, using the medium that contain 200 ng/mL lipopolysaccharide (Wuhan Saiweier Technology Co., Ltd.) 10% exosome-depleted FBS (heat-

inactivated FBS centrifuged 4°C, 100,000×g After 18 h, the lower layer of serum containing the exosomes was discarded, and 80% of the upper layer of the centrifuge tube constituted the FBS without the exosomes), and 100 U/mL penicillin-streptomycin to culture for 24 h to obtain M1 type macrophages.

Exosome isolation and characterization

RAW264.7 macrophages were cultured in an induction medium for 24 h to complete their polarization to M1 type; the induction medium was discarded, the cells were washed three times with phosphate-buffered saline (PBS), and the cells were cultured in a medium devoid of serum and antibiotics. After 24 h, the cell supernatant was collected and used to extract the exosomes.

An ultracentrifuge (Optima XE-100 Ultracentrifuge, USA) was used to perform differential ultracentrifugation to separate and purify the exosomes^[29]. First, the collected cell supernatant was centrifuged at 4°C, 3000×g for 15 min to remove cells and cell debris, and then at 12,000 ×g for 50 min to remove the microscopic particles, such as organelles, save the supernatant. The sample was then passed through a 0.22-μm filter to remove particles >200 nm. Finally, the filtered liquid was centrifuged at 4°C and 120,000 ×g for 150 min to separate the exosomes. The exosomes settled at the bottom of the six centrifuge tubes were collected, washed with PBS, and then centrifuged for 150 min at 4°C and 120,000 ×g to collect the exosomes. The small amount of the obtained precipitate contained the enriched and purified exosomes. Finally, the exosomes were resuspended in 200 μL of PBS (pH = 7.4) and stored at -80°C for later use.

ZetaView® Nanoparticle Tracking Analyzer (Particle Metrix, Meerbusch, Germany) was used to track the particle size distribution and purity of the exosomes, and HT7700 transmission electron microscope (HITACHI, Japan) was used to observe the extracted exosomes. The morphology of the exosomes was photographed, and the exosome marker protein CD9 and tumor susceptibility gene 101 (Tsg101) were identified by western blot.

Mice and animal experimental design

3-month-old female unconceived wild-type C57BL/6 mice used in this study were provided by the Experimental Animal Center of Wuhan University, and all experimental procedures were performed after obtaining approval from the Experimental Animal Welfare Ethics Committee of Wuhan University People's Hospital (Approval No. 20210306).

Establishment of a mouse SUI model^[30]: The mice were anesthetized with isoflurane (induction concentration 3–4%, maintenance concentration 1–1.5%). After disinfection and lubrication, a modified 6-Fr-Foley catheter (Dalian Couliat Medical Products Co., Ltd.), was inserted into the vagina and fixed with a 4-0 needle suture at the external mouth. This action was performed gently and did not damage the urethra or vagina of the mouse. Subsequently, 0.3 mL of normal saline was injected into the balloon

(diameter approximately equal to that of the newborn mouse's skull, i.e., 8 mm) to expand the vagina. Simultaneously, a 60-g weight was hung at the end of the catheter for traction, which was removed after 1 h. After the balloon was drained, the catheter was pulled out, and the suture was removed and disinfected.

A sneeze experiment was performed 24 h after the mice were modeled, and the mice's maximum bladder volume (MBV) and abdominal leak point pressure (ALPP) were tested to determine whether the SUI model was successful. Then, thirty-six SUI mice were randomly divided into two equal groups. One group was locally injected with M1 type macrophages-derived exosomes (M1-Exo) 1×10^{10} particles/mL, 1 mL in and around the levator ani muscle on both sides. Another group was injected with 1 mL of 0.9% normal saline locally in and around the levator ani muscle on both sides. The urodynamic parameters (MBV, ALPP) of the two groups were measured 3, 7, and 14 days after the injection ($n = 6$ at each time point).

Hematoxylin and eosin (H&E) staining

After measuring ALPP and MBV, the mice were sacrificed under anesthesia; the bilateral levator ani muscles were removed and fixed with muscle fixative (Wuhan Saiweier Biotechnology Co., Ltd.) for 24 h. The tissue specimens were embedded in paraffin, cut into 4- μ m-thick sections, and H&E staining was performed for histological observation. The BX 63 automatic microscope (Olympus, Japan) was employed to capture the morphology of the levator ani muscle.

Cyclic mechanical strain (CMS)

To calculate the CMS, 1.5 mL of suspension, with a cell density of 1×10^5 cells/mL, was taken. The C2C12 myoblast suspension in the logarithmic growth phase was spread evenly in the center of the cell strain culture plate. The plate was placed in a 100-mm cell culture dish and moved to a constant temperature incubator. The cells were allowed to adhere to the wall overnight; on the next day, the medium was changed to serum-free DMEM high glucose medium to synchronize the cell cycle to the G_0 phase. When the cell density reached about 80%, the strained culture plate covered with cells was turned upside down in the 50 mL container. A four-point bending cell mechanics loading device (Chengdu Mirui Technology Co., Ltd.) was connected to a strained petri dish holder with a volume fraction of 2% FBS and 1% penicillin-streptomycin DMEM high glucose medium.

To explore the best experimental parameters of damage to C2C12 myoblasts, the strain frequency of 1 Hz was applied and divided into three groups according to the strain force and strain time: 1333- μ strain (0 h, 4 h, 8 h, and 12 h), 2666- μ strain (0 h, 4 h, 8 h, and 12 h), and 5333- μ strain (0 h, 4 h, 8 h, and 12h). This step was followed by CCK-8 cell viability testing, and the optimal cell strain was determined to be 5333 μ . Subsequently, the senescence and apoptosis of C2C12 myoblasts were detected under the frequency of 1 Hz and strain force of 5333 μ (0 h, 4h, 8 h, and 12 h). The cyclic mechanical stress parameters that can cause significant differences in C2C12 myoblast cell activity, senescence, and apoptosis were selected as

the best injury experimental parameters, namely 1 Hz, 5333- μ strain, and 8 h. The following cell experiment was divided into three groups, namely the control group (no CMS applied injury), the applied CMS injury group (additional 1 ml of PBS solution cultured for 24 h after the applied CMS injury), and the exosome treatment group after the applied CMS injury (after CMS injury, supplementing with 1×10^{10} particles/mL, 1 mL of exosomal solution was cultured for 24 h).

Cell proliferation analysis

Cell Counting Kit-8

C2C12 myoblasts treated with different parameters and cells before and after the intervention of exosomes were trypsinized and counted on a hemocytometer to prepare a 2×10^4 /mL cell suspension. This suspension was inoculated in a 96-orifice plate (100 μ L per well, three wells in each group) and placed in an incubator at 5% CO₂ and 37°C for 30 min. After the cells adhered to the wall, 10 μ L of CCK-8 (Wuhan Kerui Biotech Co., Ltd. Company) and 90 μ L of serum-free DMEM high-glycemic culture solution were added to each well. Incubation was continued for 1 h at 37°C, 5% CO₂, and relative saturated humidity of 95%. Later, a microplate reader (Perkin Elmer, USA) was used to detect the absorbance value of each group of cells at 450 nm. The cell viability was calculated based on the average value of each group, and the experiment was repeated three times independently.

EdU incorporation assay

The C2C12 myoblasts treated with different parameters and the cells before and after the intervention of exosomes were replaced with EdU working fluid and were placed in a CO₂ incubator for 2 h. The EdU medium was discarded, 4% paraformaldehyde was added, fixed for 15 min, and then washed three times with PBS, 5 min each time. Subsequently, 1 mL of 0.3% Triton X-100 was added and incubated at room temperature for 10 min. The waste solution was discarded, 500 μ L of the click reaction solution was added, incubated at room temperature for 30 min in the dark, 0.3% Triton X-100 was added, and washed three times, 10 min each time. Hoechst 33342 staining solution was added to stain the nucleus. The images were captured using a BX 63 automatic microscope (Olympus, Japan), and ImageJ software was employed to count the number of EdU-positive cells.

Cell senescence analysis

The β -Galactosidase Staining Kit (Shanghai Biyuntian Institute of Biotechnology, China) was used to detect the degree of senescence of the C2C12 myoblasts. In this procedure, 1 mL of β -galactosidase staining fixative solution was added to the C2C12 myoblasts treated with different parameters and cells before and after the exosomal intervention. They were fixed for 15 min at room temperature, washed

three times with PBS, 5 min each time, and 1 mL of β -galactosidase staining working solution (the ratio of β -galactosidase staining solution A, B, and C and X-Gal solution was 1:1:93:5) was added. After placing overnight at 37°C in a constant temperature incubator without CO₂, the senescent cells were stained blue and were counted as positive cells. Three fields of view were randomly selected under the BX 63 automatic microscope (Olympus, Japan), and the number of positive cells was estimated. Senescence cell rate = several positive cells/the total number of cells \times 100%.

Cell apoptosis analysis

Hoechst 33258 assay

In this assay, 1 mL of fixative was added to the C2C12 myoblasts treated with different parameters and cells before and after the intervention of exosomes and fixed at room temperature for 10 min. The fixative was discarded, the strained culture plate was placed in a 100-mm sterile dish, an appropriate amount of PBS was added, and rinsed twice with slow shaking, 3 min each time. After sucking up the liquid, 1 ml Hoechst 33258 (Beyotime Biotech Co. Ltd., Shanghai, China) dye solution was added dropwise and dyed for 5 min in the dark. After sucking off the dye solution, an appropriate amount of PBS was added, exposure to light was avoided, and rinsed twice with slow shaking, 3 min each time. After mounting the slides with anti-fluorescence quenching mounting solution in the dark, the images were captured on a BX 63 automatic microscope (Olympus, Japan). The nuclei of the apoptotic cells appeared whitish and bright blue, and the number of apoptotic cells was counted using ImageJ software. Apoptotic cell rate = the number of positive cells/total number of cells \times 100%.

Flow cytometric analysis

C2C12 myoblasts treated with different parameters and cells before and after the intervention of exosomes were prepared into a suspension of 1×10^6 cells/mL; 100 μ L of the cell suspension was transferred to a 5-mL centrifuge tube, 5 μ L of PE Annexin V and 5 μ L of 7-AAD (Becton Dickinson, Franklin Lakes, NJ, USA) were added, gently vortexed, and incubated at room temperature for 15 min in the dark. Then, 400 μ L of $1 \times$ binding buffer was added to the centrifuge tube, and FACS Calibur Flow Cytometer (BD Biosciences, Franklin Lakes, NJ, USA) was used to detect cell apoptosis. The experiments were performed three times. The results were analyzed using FlowJo7.6.

Western blot analysis

The total protein of the M1 macrophages was extracted with RIPA lysis solution, and the protein concentration was determined using the BCA Protein Assay Kit (Beyotime Biotech Co. Ltd., Shanghai, China). The remaining protein solution was mixed with an appropriate amount of $5 \times$ protein loading

buffer. Appropriate amounts of the marker, exosomes, and M1 macrophages protein samples were placed in the sample wells, and they were transferred to a polyvinylidene fluoride membrane after 12% sodium dodecyl sulfate–polyacrylamide gel electrophoresis separation; 5% mass fraction skimmed milk dissolved with Tris-buffered saline with Tween (TBST) was used for 1 h at room temperature. and primary antibodies against CD9 (1:1000) and Tsg101 (1:1000) (Abcam, Cambridge, UK) were added and incubated in a shaker at 4°C; the samples were washed with TBST three times, 5 min each time. Subsequently, secondary antibodies diluted to 1:4000 at room temperature were added, incubated for 1 h, and washed with TBST three times, 5 min each time. The Li-Cor Odyssey Infrared Imaging System (Li-Cor Biosciences, Lincoln, NE, USA) was used to detect protein expression and identify the exosomes.

Statistical analysis

GraphPad Prism 8.0 software (GraphPad, San Diego, CA, USA) was used to analyze the experimental results. The measured data were expressed as mean \pm SEM. One-way analyses of variance (ANOVA) were applied to compare the differences between the groups. $p < 0.05$ was considered a statistically difference. $p < 0.01$ and $p < 0.001$ were regarded as significant differences.

Abbreviations

SUI Stress urinary incontinence

CMS Cyclic mechanical strain

VD Vaginal dilation

CCK-8 Cell Counting Kit-8

M1-Exo Exosomes secreted by M1 type macrophages

ALPP Abdominal leak point pressure

MBV Maximum bladder volume

Declarations

Ethics approval and consent to participate

All procedures involving animals were approved by the Experimental Animal Center of Wuhan University and all experimental procedures were performed after obtaining approval from the Experimental Animal Welfare Ethics Committee of Wuhan University People's Hospital (Approval No. 20210306).

Consent for publication

Not applicable.

Availability of data and materials

The data that support the findings of this study are available from the corresponding authors upon reasonable request.

Competing interests

None.

Funding

This work was supported by the National Natural Science Foundation of China (no. 81971364 and 81771562), The National Key R&D Program of China [2018YFC2002204] The Second Medical Leading Talents Project of Hubei Province (no. [2019]47).

Acknowledgments

The authors would like to thank all the staff in the Experimental Animal Center of Wuhan University and Central Laboratory of Wuhan University, for their technical assistance.

Authors' contributions

Jianhong Cheng and Shasha Hong contributed equally. Jianhong Cheng and Hong Shasha: Design experiments, Experiments, Analyze data, and write a paper. Lian Yang: Urodynamic measurement in mice (ALPP MBV); Jianfeng Liu: mouse modeling, tissue sampling of mice and data collection; Li Hong: conceptualization, funding acquisition, and final approval.

References

1. Kalejaiye O, Vij M, Drake MJ. Classification of stress urinary incontinence[J]. *World J Urol*. 2015;33(9):1215–20.
2. Thomason AD, Miller JM, Delancey JO. Urinary incontinence symptoms during and after pregnancy in continent and incontinent primiparas[J]. *Int Urogynecol J Pelvic Floor Dysfunct*. 2007;18(2):147–51.
3. Daly D, Clarke M, Begley C. Urinary incontinence in nulliparous women before and during pregnancy: prevalence, incidence, type, and risk factors[J]. *Int Urogynecol J*. 2018;29(3):353–62.

4. Sangsawang B, Sangsawang N. Stress urinary incontinence in pregnant women: a review of prevalence, pathophysiology, and treatment[J]. *Int Urogynecol J*. 2013;24(6):901–12.
5. Martinho N, Friedman T, Turel F, et al. Birthweight and pelvic floor trauma after vaginal childbirth[J]. *Int Urogynecol J*. 2019;30(6):985–90.
6. Spiller KL, Koh TJ. Macrophage-based therapeutic strategies in regenerative medicine[J]. *Adv Drug Deliv Rev*. 2017;122:74–83.
7. Chen P, Piao X, Bonaldo P. Role of macrophages in Wallerian degeneration and axonal regeneration after peripheral nerve injury[J]. *Acta Neuropathol*. 2015;130(5):605–18.
8. Schlundt C, El KT, Serra A, et al. Macrophages in bone fracture healing: Their essential role in endochondral ossification[J]. *Bone*. 2018;106:78–89.
9. Chazaud B. Inflammation and Skeletal Muscle Regeneration: Leave It to the Macrophages![J]. *Trends Immunol*. 2020;41(6):481–92.
10. Saclier M, Cuvellier S, Magnan M, et al. Monocyte/macrophage interactions with myogenic precursor cells during skeletal muscle regeneration[J]. *FEBS J*. 2013;280(17):4118–30.
11. Arnold L, Henry A, Poron F, et al. Inflammatory monocytes recruited after skeletal muscle injury switch into antiinflammatory macrophages to support myogenesis[J]. *J Exp Med*. 2007;204(5):1057–69.
12. Kalluri R, LeBleu VS. The biology, function, and biomedical applications of exosomes[J]. *Science*, 2020,367(6478).
13. Zhang Y, Liu Y, Liu H, et al. Exosomes: biogenesis, biologic function and clinical potential[J]. *Cell Biosci*. 2019;9:19.
14. Meldolesi J. Exosomes and Ectosomes in Intercellular Communication[J]. *Curr Biol*. 2018;28(8):R435–44.
15. Jiang M, Liu J, Liu W, et al. Bone marrow stem cells secretome accelerates simulated birth trauma-induced stress urinary incontinence recovery in rats[J]. *Aging*. 2021;13(7):10517–34.
16. Memon HU, Blomquist JL, Dietz HP, et al. Comparison of levator ani muscle avulsion injury after forceps-assisted and vacuum-assisted vaginal childbirth[J]. *Obstet Gynecol*. 2015;125(5):1080–7.
17. Dietz HP, Franco AV, Shek KL, et al. Avulsion injury and levator hiatal ballooning: two independent risk factors for prolapse? An observational study[J]. *Acta Obstet Gynecol Scand*. 2012;91(2):211–4.
18. Dietz HP, Scoti F, Subramaniam N, et al. Impact of subsequent pregnancies on pelvic floor functional anatomy[J]. *Int Urogynecol J*. 2018;29(10):1517–22.
19. Blomquist JL, Carroll M, Munoz A, et al. Pelvic floor muscle strength and the incidence of pelvic floor disorders after vaginal and cesarean delivery[J]. *Am J Obstet Gynecol*. 2020;222(1):61–2.
20. Dietz HP, Steensma AB. The prevalence of major abnormalities of the levator ani in urogynaecological patients[J]. *BJOG*. 2006;113(2):225–30.
21. Luginbuehl H, Lehmann C, Baeyens JP, et al. Involuntary reflexive pelvic floor muscle training in addition to standard training versus standard training alone for women with stress urinary

- incontinence: study protocol for a randomized controlled trial[J]. *Trials*. 2015;16:524.
22. Robinson D, Cardozowan L. Urinary incontinence in the young woman: treatment plans and options available[J]. *Womens Health (Lond)*. 2014;10(2):201–17.
 23. Jovan HD, Uros B, Aleksandar A, et al. Etiopathogenesis, diagnostics and history of surgical treatment of stress urinary incontinence[J]. *Acta Chir Iugosl*. 2014;61(1):85–90.
 24. Pegtel DM, Gould SJ. Exosomes[J] *Annu Rev Biochem*. 2019;88:487–514.
 25. Wu P, Zhang B, Shi H, et al. MSC-exosome: A novel cell-free therapy for cutaneous regeneration[J]. *Cytherapy*. 2018;20(3):291–301.
 26. Soares MT, Trindade D, Vaz M, et al. Diagnostic and therapeutic potential of exosomes in Alzheimer's disease[J]. *J Neurochem*. 2021;156(2):162–81.
 27. Holliday LS, McHugh KP, Zuo J, et al. Exosomes: novel regulators of bone remodelling and potential therapeutic agents for orthodontics[J]. *Orthod Craniofac Res*. 2017;20(Suppl 1):95–9.
 28. Zhao X, Ren Y, Lu Z. Potential diagnostic and therapeutic roles of exosomes in pancreatic cancer[J]. *Biochim Biophys Acta Rev Cancer*. 2020;1874(2):188414.
 29. Wang Z, Zhu H, Shi H, et al. Exosomes derived from M1 macrophages aggravate neointimal hyperplasia following carotid artery injuries in mice through miR-222/CDKN1B/CDKN1C pathway[J]. *Cell Death Dis*. 2019;10(6):422.
 30. Catanzarite T, Bremner S, Barlow CL, et al. Pelvic muscles' mechanical response to strains in the absence and presence of pregnancy-induced adaptations in a rat model[J]. *Am J Obstet Gynecol*. 2018;218(5):511–2.

Figures

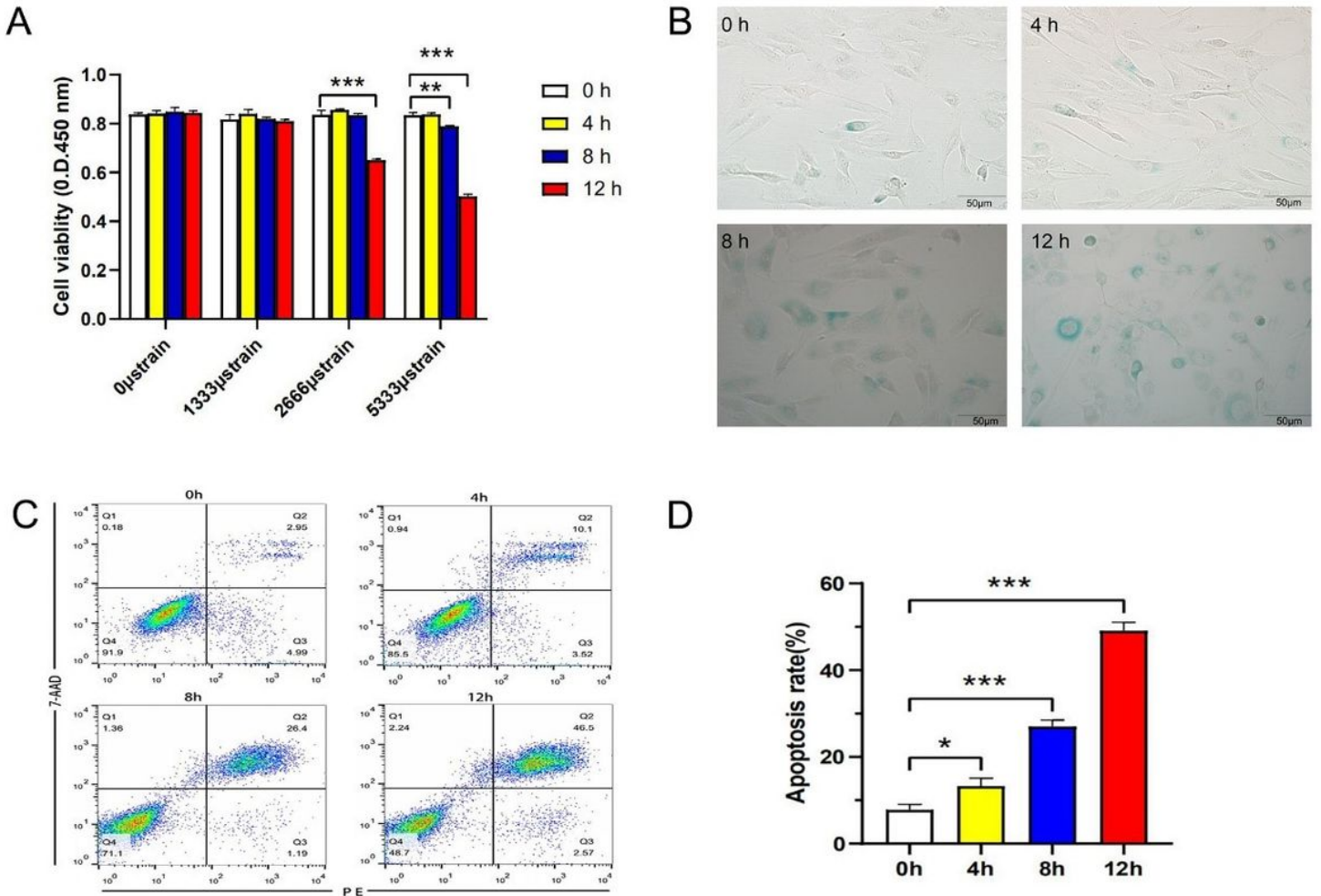


Figure 1

The effects of cyclic mechanical strain (CMS) on C2C12 myoblasts activity. A. The effect of cyclic mechanical strain (1 Hz) on C2C12 myoblasts viability. B. The effect of cyclic mechanical strain (1 Hz, 5333-μ strain) on the senescence of C2C12 myoblasts, Scale bar = 50 μm. C. The effect of cyclic mechanical strain (1 Hz, 5333-μ strain) on the apoptosis of C2C12 myoblasts. D. Quantitative statistics of the effect of mechanical force on the apoptosis of C2C12 myoblasts (8 h, 1 Hz, 5333-μ strain). 0 h, 4 h, 8 h, and 12 h represent that the C2C12 myoblast stretched for 0 h, 4 h, 8 h, and 12 h, respectively. The values presented are mean ± SEM (n = 3), *P < 0.05 **P < 0.01 ***P < 0.001.

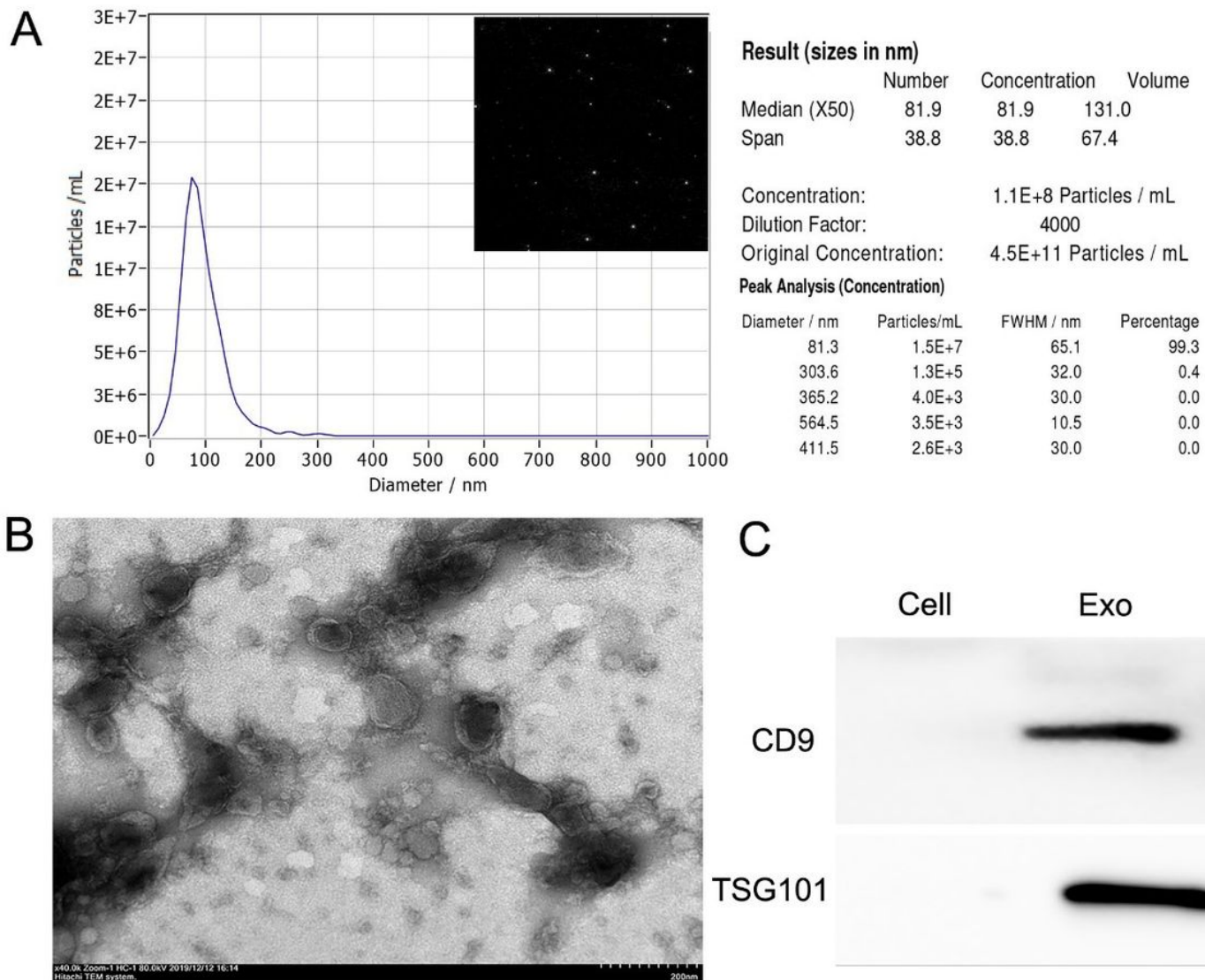


Figure 2

The characterizations of exosomes derived from M1-type macrophages. A. Nanoparticle tracking analysis measurements of the concentration and size distribution of isolated M1-type macrophages-derived exosomes. B. Transmission electron microscopy TEM image of M1-type macrophages-derived exosomes, Scale bar = 200 nm. C. Western blot analysis showing anti-CD9 and anti-tumor susceptibility gene 101 (Tsg101) of 40 µg of exosome lysates derived from M1-type macrophages.

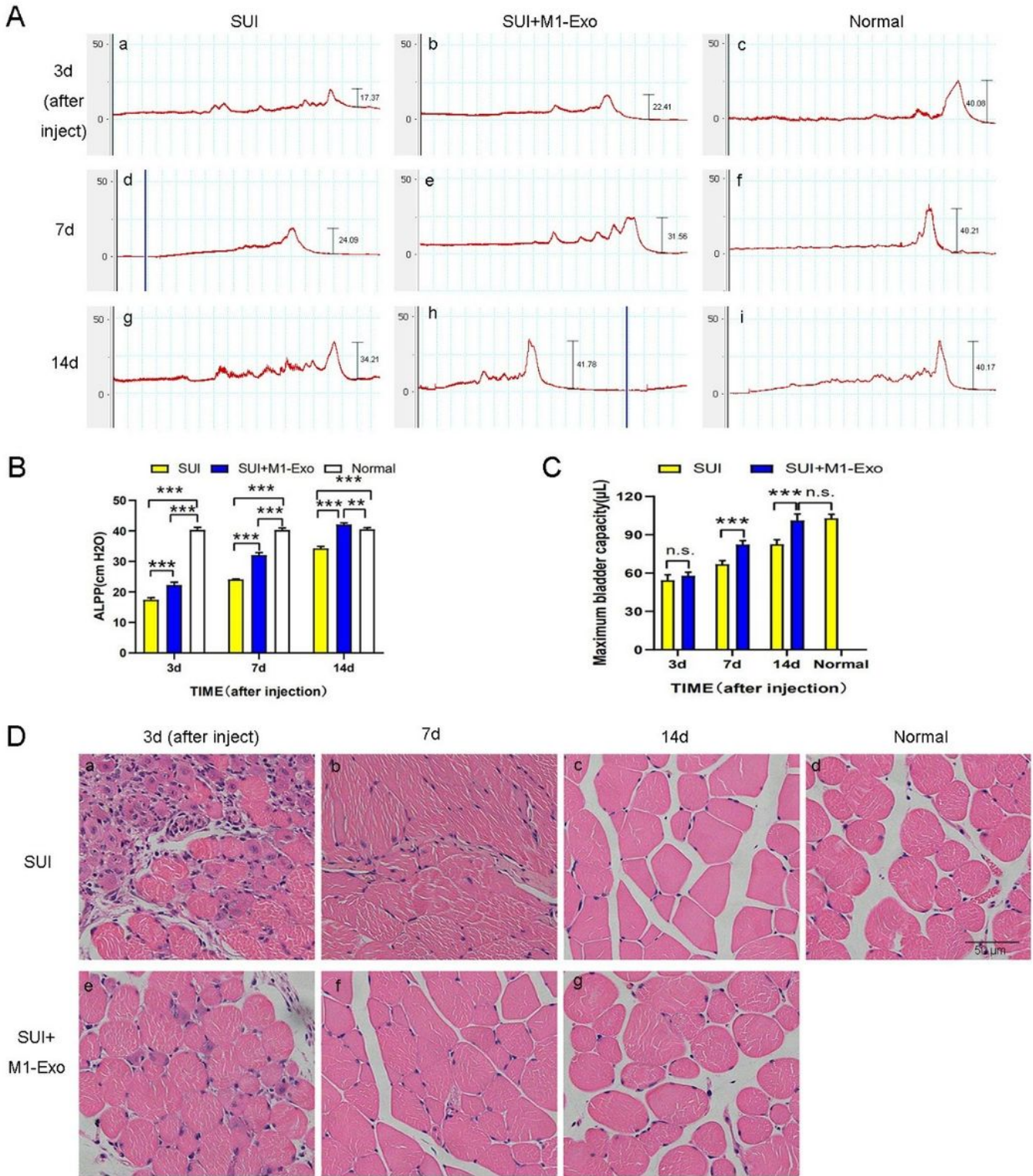


Figure 3

M1- Exo promote the repair of the levator ani in SUI mice and improve the urodynamic parameters. A. The Powerlab software measures ALPP and MBV of mice 3, 7, and 14 days after M1-Exo and saline injection. B. ALPP statistical results. C. MBV statistical results. D. H&E staining of the levator ani muscle. * $P < 0.05$ ** $P < 0.01$ *** $P < 0.001$; N.S., no significance

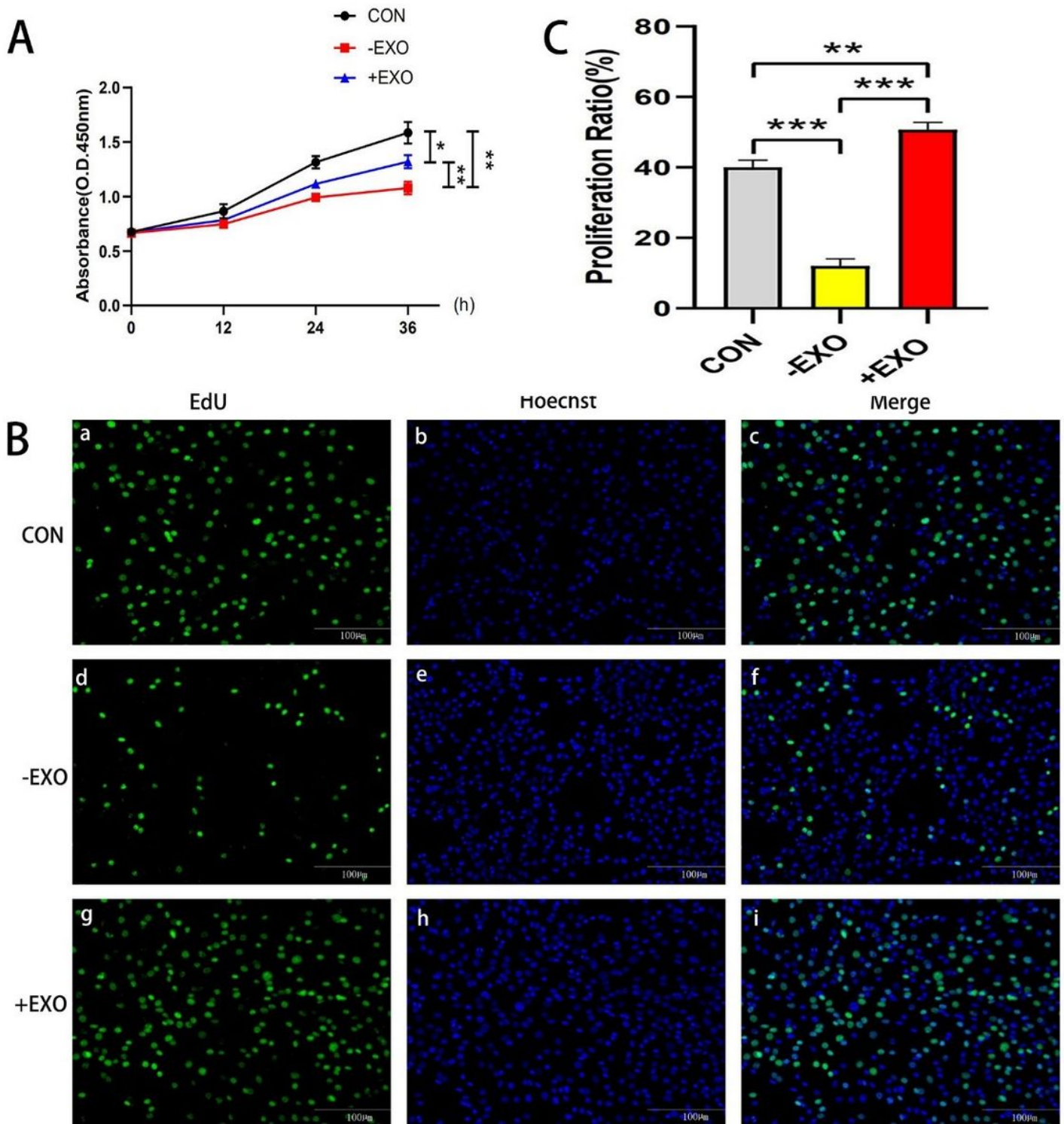


Figure 4

The effect of M1-Exo on the proliferation of C2C12 myoblasts injured by CMS. A. CCK-8 detects the activity of 3 groups of C2C12 myoblasts (CON, -EXO, +EXO) damaged by mechanical force. CON: The normal uninjured group; -EXO: M1-type macrophages-derived exosomes without intervention in mechanically induced injury the C2C12 myoblast group; +EXO: M1-type macrophages exosomes interfered with mechanically induced injury the C2C12 myoblast group. B. Edu staining to detect the

proliferation of C2C12 myoblasts injured by mechanical force in the 3 groups. C. Perform quantitative statistics on Figure D. The results indicate the mean \pm SEM (n = 3), *P < 0.05 **P < 0.01 ***P < 0.001.

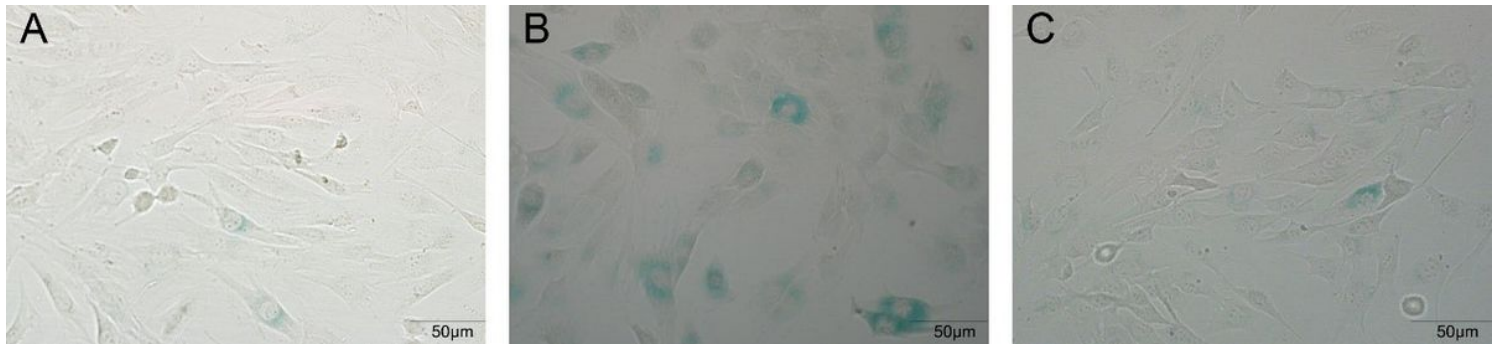


Figure 5

The effect of M1-Exo on the senescence of C2C12 myoblasts after the induction of mechanical trauma. Cell senescence was determined with a senescence-associated beta-galactosidase (SA- β -Gal) staining assay. A. Control group; B. C2C12 myoblast injury group cultured with vehicle solution; C. C2C12 myoblast injury group cultured with M1-Exo. Bar = 50 μ m.

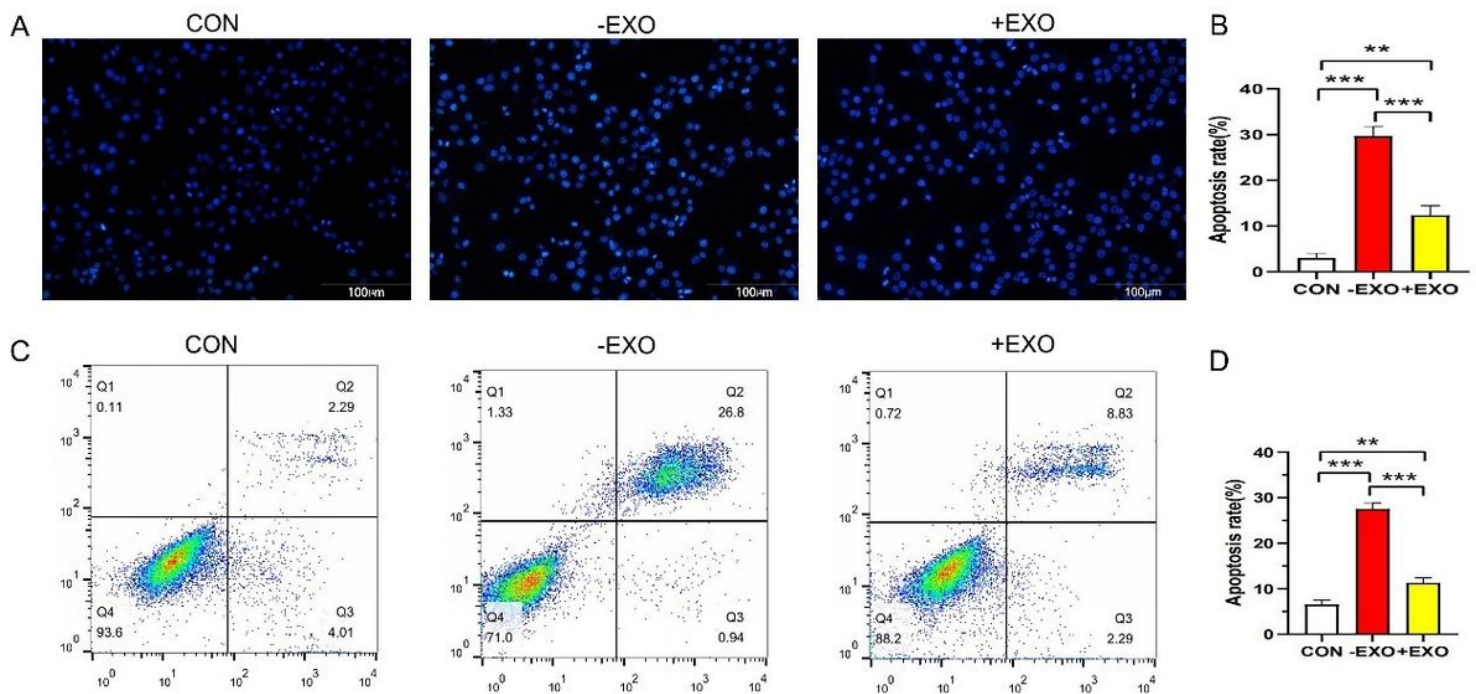


Figure 6

The effect of M1-Exo on the apoptosis of C2C12 myoblasts after the induction of mechanical injury. A. Hoechst 33258 staining to detect cell apoptosis, magnification \times 100; apoptosis rate = the number of apoptotic cells/total cells. B. Annexin V-PE/7-AAD double staining flow cytometry to detect cell apoptosis. The values presented are the mean \pm SEM (n = 3), *P < 0.05 **P < 0.01 ***P < 0.001.